www.czasopisma.pan.pl PAN POLSKA AKADEMIA NAUK www.journals.pan.pl

PAN ARCHIVES OF ACOUSTICS
Vol. 41, No. 1, pp. 43–53 (2016)



DOI: 10.1515/aoa-2016-0004

# Shape Optimisation of Multi-Chamber Acoustical Plenums Using BEM, Neural Networks, and GA Method

Ying-Chun CHANG[(1)], Ho-Chih CHENG[(2)], Min-Chie CHIU[(2)], Yuan-Hung CHIEN[(1)]

[(1)] *Department of Mechanical Engineering, Tatung University*
Taiwan, ROC

[(2)] *Department of Mechanical and Automation Engineering, Chung Chou University of Science and Technology*
No. 6, Lane 2, Sec.3, Shanchiao Rd., Yuanlin, Changhua 51003, Taiwan, ROC; e-mail: minchie.chiu@msa.hinet.net

(*received May 21, 2015; accepted October 14, 2015*)

Research on plenums partitioned with multiple baffles in the industrial field has been exhaustive. Most researchers have explored noise reduction effects based on the transfer matrix method and the boundary element method. However, maximum noise reduction of a plenum within a constrained space, which frequently occurs in engineering problems, has been neglected. Therefore, the optimum design of multi-chamber plenums becomes essential. In this paper, two kinds of multi-chamber plenums (Case I: a two-chamber plenum that is partitioned with a centre-opening baffle; Case II: a three-chamber plenum that is partitioned with two centre-opening baffles) within a fixed space are assessed.

In order to speed up the assessment of optimal plenums hybridized with multiple partitioned baffles, a simplified objective function (OBJ) is established by linking the boundary element model (BEM, developed using SYSNOISE) with a polynomial neural network fit with a series of real data – input design data (baffle dimensions) and output data approximated by BEM data in advance. To assess optimal plenums, a genetic algorithm (*GA*) is applied. The results reveal that the maximum value of the transmission loss (*TL*) can be improved at the desired frequencies. Consequently, the algorithm proposed in this study can provide an efficient way to develop optimal multi-chamber plenums for industry.

**Keywords:** boundary element method; plenum; centre-opening baffle; polynomial neural network model; group method of data handling; optimisation; genetic algorithm.

## Notations

Throughout the paper the following notations are used:

$bit$ – bit length of chromosome,
$iter_{\max}$ – maximum iteration during *GA* optimisation,
$L_1$, $L_2$ – design parameters of a two-chamber plenum [m],
$LL_1$, $LL_2$ – design parameters of a three-chamber plenum [m],
$pc$ – crossover ratio,
$pm$ – mutation ratio,
$pop$ – number of population,
$TL$ – sound transmission loss [dB].

## 1. Introduction

Noise control work on venting noise that uses an acoustical plenum in industry is vital (Alley *et al.*, 1989; Cheremisinoff, 1977). The research on acoustical plenums has been widely discussed. Ko (1971) started the study of sound transmission loss (*TL*) for a rectangular tube with both upper and lower sides internally lined with perforated sound absorbing material. On the basis of linear acoustic theory, Blair and Coate (1972) assessed the *TL* of a venting system. Later, McCormick (1975) proposed a sound attenuation loss of a two-sided and four-sided rectangular tube lined with sound absorbing material. At the same time, Efowcs and Howe (1975) analysed the influence of noise reduction with respect to different flowing rates. Bies and Hansen (1988) also assessed the *TL* of a one-chamber plenum internally lined with sound absorbing material. Munjal (1997) analysed the acoustical performance of a side inlet/outlet plenum using the plane wave theory. Li and Hansen (2005) assessed the acoustical performance of a rectangular plenum using theoretical and experimental data in 2005. Later, Liu and Herrin (2009) analysed the influence of the plenum's acoustical performance with respect to the perforated hole's distance using a finite element method.

In practical engineering work, there is a growing need to optimize the acoustical performance within

a limited space. Yet, the need to investigate the optimal acoustical plenum within a constrained space is rarely approached. In previous work (Chang *et al.*, 2004; Yeh *et al.*, 2004; Chang *et al.*, 2005a; Yeh *et al.*, 2006), the shape optimisations of reactive mufflers have been discussed using a simple theoretical model in conjunction with a genetic algorithm (*GA*). However, the mathematical model for a multi-chamber plenum lined with sound absorbing material is complicated and time-consuming. In order to speed up the optimisation process, a simplified objective function (*OBJ*) established by linking the boundary element model (*BEM*) with the polynomial neural network model (*NNM*) is optimised using the *GA*. In this paper, two kinds of multi-chamber acoustical plenums (those hybridized with two and three chambers as shown in Fig. 1) used in reducing various targeted tones (400, 800, and 1200 Hz) are discussed.

a) two-chamber plenum

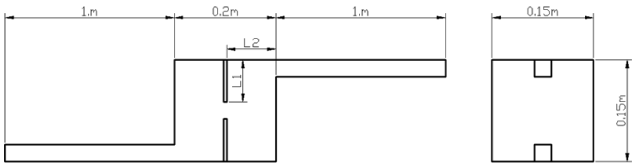


b) three-chamber plenum

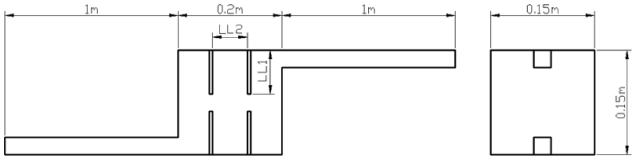


Fig. 1. Dimensions for two kinds of multi-chamber plenums: a) a two-chamber plenum partitioned with a centre-opening baffle; b) a three-chamber plenum partitioned with two centre-opening baffles.

## 2. Neural Network Model (NNM)

The main advantage of neural networks lies in their ability to represent both linear and non-linear relationships as well as to learn these relationships directly from the data being modelled. The most common neural network model is the multilayer perceptron (*MLP*) which requires a desired output in order to learn. In this paper, a well-known polynomial neural network used in optimisation is adopted and discussed.

### *2.1. Concept of the Polynomial Neural Network*

Artificial Neural Networks (*ANN*) have been successfully applied in many fields to model complex non-linear relationships. *ANN*s may be viewed as the universal approximators, but there is a disadvantage: detected dependencies are hidden within the neural network structure. A polynomial neural network called the Group Method of Data Handling (*GMDH*) was also developed by Ivakhnenko (1971) while working on an improved method for predicting fish populations in rivers. Ivakhnenko made the neuron a more complex unit that featured a polynomial transfer function. The interconnections between layers of neurons were simplified, and an automatic algorithm for structure design and weight adjustment was developed. The main idea of *GMDH* is to use feedforward networks based on short-term polynomial transfer functions whose coefficients are obtained using regression techniques combined with emulating self-organizing activities for neural network (*NN*) structural learning. The polynomial neural network is a self-organizing adaptive model which can establish a relationship between input and output parameters. The polynomial network is used for recognition in a non-linear system.

The *GMDH* algorithm, a self-organized recognition method in a nonlinear system, can establish an adaptive, monitoring, or learning model. By using monitoring and learning at input and output, the output data is modelled by the input function.

### *2.2. Polynomial Neural Network built up*

As indicated in Fig. 2, the polynomial neural network is composed of an input layer, a hidden layer $\Sigma$(summation), and an output layer (product), where the hidden layer is the weight summation, the output layer is the product of the input and weighted value, and $w_{nk}$ is the weighted value (Patrikar, Provence, 1996). Therefore, the $j$-th output $z_{jk}$ is

$$z_{jk} = \sum_{i=0}^{n} w_{ij} x_{ik}. \tag{1}$$

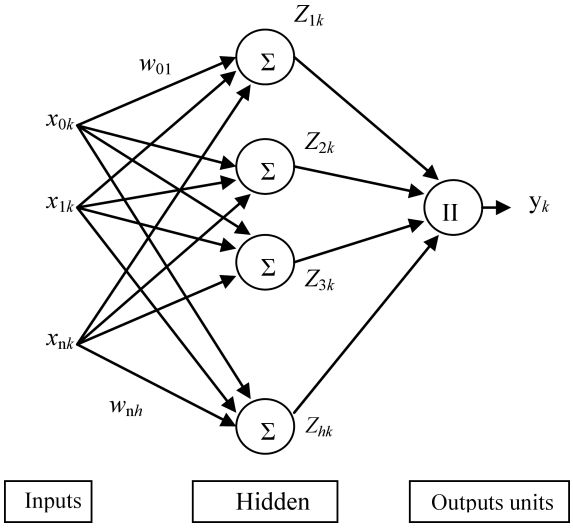


Fig. 2. Organisation of a polynomial neural network.

The total output of the neural network is expressed as

$$y_k = \prod_{j=1}^{h} z_{jk}, \tag{2}$$

where $h$ is the unit's number in a hidden layer.

Combining Eqs. (1), (2) yields

$$y_k = B_0 + \sum_{i=1}^{n} B_i x_i + \sum_{i=1}^{n}\sum_{j=1}^{n} B_{ij} x_i x_j + ... + \sum_{i=1}^{n}\sum_{j=1}^{n} ... \sum_{k=1}^{n} B_{ij...k} x_i x_j ... x_k, \tag{3}$$

where $y_k$ is the output value, $x_i$, $x_j$, $x_k$ are the input data, and $B_0$, $B_i$, $B_{ij}$, and $B_{ijk}$ are the coefficients of the node function.

### 2.3. System training on NNM

To obtain the *NNM* using the theoretical data of the *BEM* as the input data (plenum dimensions such as $L_1$, $L_2$, $LL_1$, and $LL_2$) and the output data ($TL$) in the proposed *NNM*, a trained *NNM* can be achieved using the training data bank and polynomial calculation of the *PSE* standard (deviation of the mean square).

*PSE* is expressed as

$$PSE = FSE + k_p, \tag{4}$$

$$FSE = \frac{1}{N}\sum_{i=1}^{N} (\widehat{y}_i - y_i)^2, \tag{5}$$

where *FSE* is the deviation of the mean square, $k_p$ is the penalty function, $N$ is the amount of training data, $\widehat{y}_i$ is the required data, and $y_i$ is the predicted data for *NNM*.

The penalty function $k_p$ can be expressed as

$$k_p = CPM\frac{2\sigma p^2 Q}{N}, \tag{6}$$

where *CPM* is the product of the penalty function, $Q$ is the number of the network's coefficients, and $\sigma p^2$ is the error variation.

The steps of the *NNM* construction shown in Fig. 3 include the following:

(A) Building up the data bank for network training.
The data bank is used to construct a polynomial neural network. It can be divided into two parts – the training data and the testing data. The former is adopted for the training of the *NNM*, while the latter is used for evaluating the *NNM*.

(B) Building up the neural network model.
By selecting the number and type of layers and using the training data bank in the chosen network, the neural network model can be built.

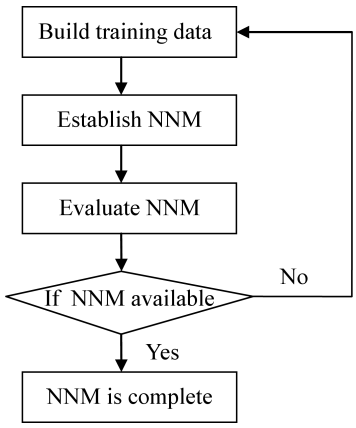


Fig. 3. Steps in the NNM.

(C) Evaluating the ability of the *NNM*.
After the *NNM* is established, a function test with testing data is required for evaluating the ability of the *NNM*.

(D) Using the *NNM*
The predicted *TL* can be obtained by inputting arbitrary design data. The *NNM*, an *OBJ* function, is used along with the *GA* optimiser during the optimisation process.

## 3. Accuracy check

### 3.1. BEM model

We use SYSNOISE package to assess the BEM's noise simulation. A speaker sound source shown in Fig. 4 is adopted. With this, only the outline shell of the plenum is meshed and the acoustical pressures at the nodes can be quickly assessed. The BEM method can save the simulation time.

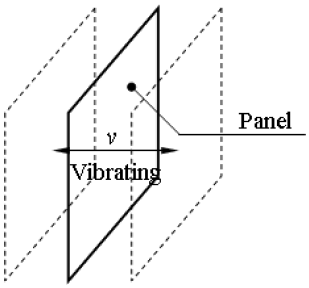


Fig. 4. Speaker sound source used in the BEM (SYSNOISE package).

Before performing the *GA* optimal simulation on plenums, an accuracy check of the mathematical model of the *BEM* on the fundamental element for a three-chamber plenum shown in Fig. 5 was performed using experimental data. As revealed in Fig. 5, the *BEM* and experimental data for the three-chamber plenum are roughly in agreement. Consequently, the developed

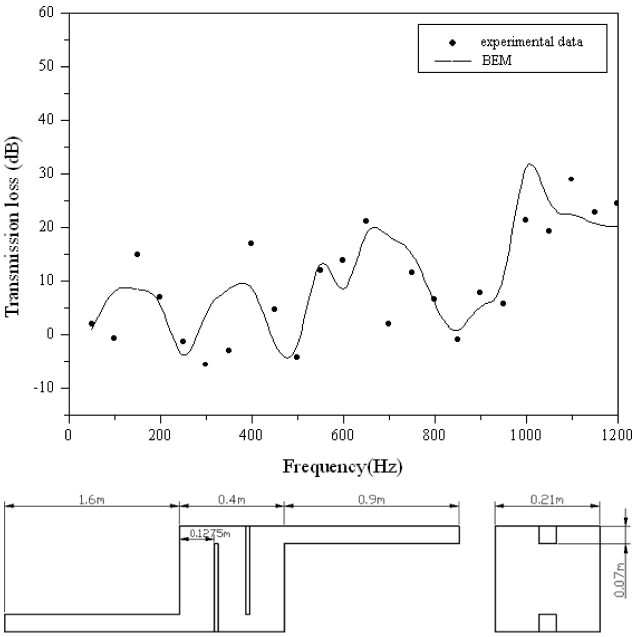


Fig. 5. Accuracy of a BEM theory used in a three-chamber plenum using experimental data.

*BEM* model for two kinds of multi-chamber plenums (a two-chamber and a three-chamber) linked by the numerical method is applied to the shape optimisation in the following section.

### *3.2. NNM model*

Sixteen training data sets used in a two-chamber plenum (Case I) and a three-chamber plenum (Case II) are shown in Table 1 and Table 2. These data sets

Table 1. Training data sets used for establishing the NNM (Case I).

| Design data set | $L_1$ | $L_2$ |
|---|---|---|
| 1 | 0.075 | 0.085 |
| 2 | 0.075 | 0.095 |
| 3 | 0.075 | 0.105 |
| 4 | 0.075 | 0.115 |
| 5 | 0.085 | 0.085 |
| 6 | 0.085 | 0.095 |
| 7 | 0.085 | 0.105 |
| 8 | 0.085 | 0.115 |
| 9 | 0.115 | 0.085 |
| 10 | 0.115 | 0.095 |
| 11 | 0.115 | 0.105 |
| 12 | 0.115 | 0.115 |
| 13 | 0.125 | 0.085 |
| 14 | 0.125 | 0.095 |
| 15 | 0.125 | 0.105 |
| 16 | 0.125 | 0.115 |

Table 2. Training data sets used for establishing the NNM (Case II).

| Design data set | $LL_1$ | $LL_2$ |
|---|---|---|
| 1 | 0.075 | 0.05 |
| 2 | 0.075 | 0.06 |
| 3 | 0.075 | 0.07 |
| 4 | 0.075 | 0.08 |
| 5 | 0.085 | 0.05 |
| 6 | 0.085 | 0.06 |
| 7 | 0.085 | 0.07 |
| 8 | 0.085 | 0.08 |
| 9 | 0.115 | 0.05 |
| 10 | 0.115 | 0.06 |
| 11 | 0.115 | 0.07 |
| 12 | 0.115 | 0.08 |
| 13 | 0.125 | 0.05 |
| 14 | 0.125 | 0.06 |
| 15 | 0.125 | 0.07 |
| 16 | 0.125 | 0.08 |

are used for establishing the *NNM* models. Before using the *NNM* as an *OBJ* function in the *GA* optimisation, an accuracy check of the *NNM* is performed by validating the data sets. As indicated in Table 3, for a two-chamber plenum partitioned with a baffle (Case I), the errors between *NNM* and *BEM* at the targeted tones (400 Hz, 800 Hz, and 1200 Hz) are 0.5%, 13%, and 6.2%. Similarly, as indicated in Table 4, the errors between *NNM* and *BEM* at the targeted tones (400 Hz, 800 Hz, and 1200 Hz) are 5.1%, 14.1%, and 10.1%. Therefore, the *NNM* serving as an objective function for the multi-chamber plenum is acceptable.

Table 3. Validation data sets used for establishing the NNM (Case I).

| Target frequency | $L_1$ | $L_2$ | BEM | NNM | error [%] |
|---|---|---|---|---|---|
| 400 | 0.0375 | 0.0853 | 12.19 | 12.26 | 0.5 |
| 800 | 0.061 | 0.1013 | 18.15 | 20.76 | 13 |
| 1200 | 0.0598 | 0.1150 | 13.21 | 14.08 | 6.2 |

Table 4. Validation data sets used for establishing the NNM (Case II).

| Target frequency | $LL_1$ | $LL_2$ | BEM | NNM | error [%] |
|---|---|---|---|---|---|
| 400 | 0.0375 | 0.0736 | 11.42 | 12.04 | 5.1 |
| 800 | 0.05365 | 0.0501 | 15.38 | 17.92 | 14.1 |
| 1200 | 0.0625 | 0.0815 | 20.37 | 22.66 | 10.1 |

## 4. Genetic algorithm

Various methods used for solving optimisation problems can be classified as enumerative, deterministic and stochastic. The first techniques are satisfactory for solving problems that are defined by a few discrete decision variables only (Laurence, 1998; Rardin, 1998) The second technique integrates the problem domain knowledge and reduces the size of the search space. However, the gradient method, one of the deterministic techniques, requires a starting point or a mathematical derivation that is calculated in advance during the optimisation process (Chang *et al.*, 2005b). Evolutionary Algorithms (*EA*s) belong to the group of stochastic search methods, also referred to as random search. Evolutionary Algorithms have been widely developed during the last two decades. Many good *EA*s have been established

A genetic algorithm (*GA*), a robust scheme used to search for the global optimum by imitating a genetic evolutionary process, first formalized by Holland (1975) and later extended to functional optimisation by Jong (1975), has been widely used in various fields (Chiu, Chang, 2008; 2010; Chiu, 2010). The *GA* provides an efficient search in complex spaces. Survival of the fittest "genes" and structured randomized genetic operations are the important ideas. The main advantages of the *GA* include the following: (1) solutions coded as bit strings (chromosomes) in which large problems can be easily handled by using long strings; (2) genetic operations, such as crossover, mutation, and elitism, are very easy to implement; (3) a mating pool of chromosomes.

In this paper, for the optimisation of the objective function (*OBJ*), the design parameters of $(X_1, X_2, \ldots, X_k)$ were determined. When the bit (the bit length of the chromosome) and the pop (population number) were chosen, the interval of the design parameter $(X_k)$ with $[Lb, Ub]_k$ was then mapped to the band of the binary value. The initial population was built up by randomisation. The parameter set was encoded to form a string which represented the chromosome. By evaluating the objective function (*OBJ*), the whole set of chromosomes $[B2D_1, B2D_2, \ldots, B2D_k]$ that changed from binary to decimal form was then assigned a fitness by decoding the transformation system. As indicated in Fig. 6, during the *GA* optimisation, one pair of offsprings was generated from the selected parent using a uniform crossover with the probability of *pc*. Genetically, mutation occurred with the probability of *pm* where the new and unexpected point was brought into the *GA*'s optimiser search domain. To prevent the best gene from disappearing and to improve the accuracy of optimisation during reproduction, the elitism scheme of keeping the best gene (one pair) in the parent generation using a tournament strategy was developed. The process was terminated when the number of generations exceeded a preselected value of $iter_{\max}$. The block diagram of the *GA* optimisation on mufflers is depicted in Fig. 7.

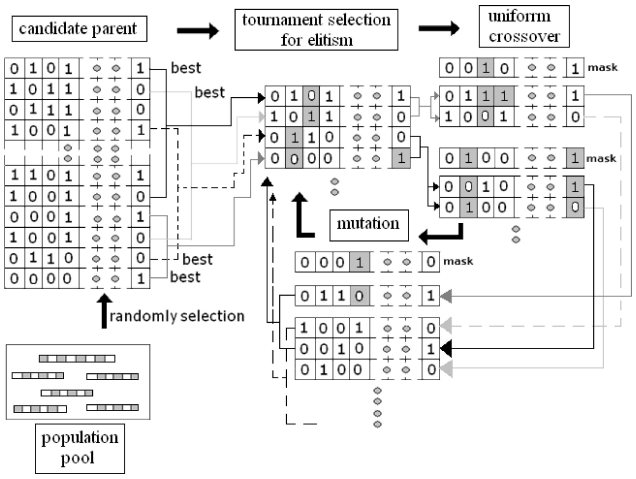


Fig. 6. Operations of the *GA* method.

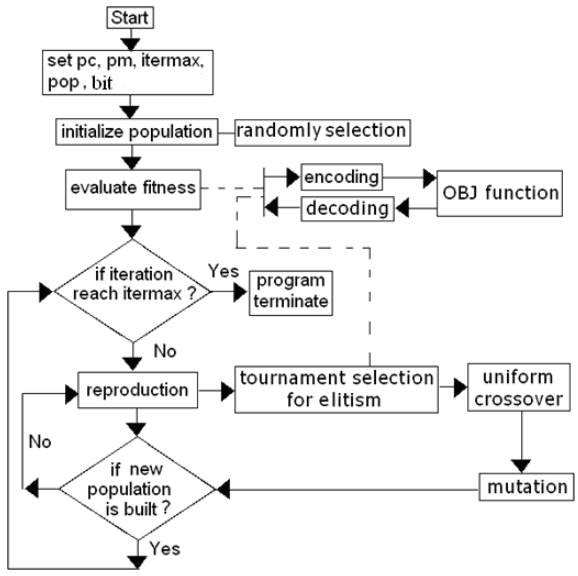


Fig. 7. Flow chart of the *GA*.

## 5. Case studies

In this paper, the original plenums (a two-chamber and three-chamber plenum) shown in Fig. 1 are introduced. To achieve a higher acoustical performance (*TL*), two kinds of cases with different design parameter sets are exemplified below.

### *5.1. CASE I: A two-chamber plenum partitioned with a centre-opening baffle*

As indicated in Fig. 1a, to simplify the optimisation, it is assumed that two baffles located at a distance of $L_2$ from the right end and with a depth of $L_1$ are in symmetry. To appreciate the acoustical performance

within a limited space, two kinds of design parameters – $L_1$ and $L_2$ – are chosen as the tuned variables. Therefore, the *TL* with respect to sixteen training data sets shown in Table 1 is calculated by the *BEM*. Using $L_1$ and $L_2$ as the input data and the *TL* as the output data in the *NNM*, and inputting a series of training data into the *NNM* system, the fitness functions of the targeted frequencies (400 Hz, 800 Hz, and 1200 Hz) are established and shown below.

**A. Target frequency – 400 Hz**

$$
\begin{aligned}
N1_{400} &= -4.69668 + 46.9668 \times L_1,\\
N2_{400} &= -8.22724 + 216.506 \times L_2,\\
N3_{400} &= 0.0783477 - 1.78184 \times N1_{400}\\
&\quad + 0.0241364 \times N2_{400} + 0.167665 \times N1_{400}^2\\
&\quad + 0.0840945 \times N2_{400}^2\\
&\quad + 0.00747251 \times N1_{400} \times N2_{400}\\
&\quad + 0.774918 \times N1_{400}^3 - 0.224627 \times N2_{400}^3,\\
TL_{400} &= 14.2169 + 10.5154 \times N3_{400}.
\end{aligned}
\tag{7}
$$

**B. Target frequency – 800 Hz**

Similarly, the fitness function of the targeted frequency (800 Hz) is established and shown in Eq. (8).

$$
\begin{aligned}
N1_{800} &= -4.69668 + 46.9668 \times L_1,\\
N2_{800} &= -8.22724 + 216.506 \times L_2,\\
N3_{800} &= 0.191423 + 1.34789 \times N1_{800}\\
&\quad - 0.0763915 \times N2_{800} - 0.0992282\\
&\quad \times N1_{800}^2 - 0.104956 \times N2_{800}^2\\
&\quad + 0.0291079 \times N1_{800} \times N2_{800}\\
&\quad - 0.354633 \times N1_{800}^3\\
&\quad + 0.0449907 \times N2_{800}^3,\\
TL_{800} &= 7.92746 + 11.7688 \times N3_{800}.
\end{aligned}
\tag{8}
$$

Likewise, the fitness function of the targeted frequency (1200 Hz) is established and shown in Eq. (9).

$$
\begin{aligned}
N1_{1200} &= -4.69668 + 46.9668 \times L_1,\\
N2_{1200} &= -8.22724 + 216.506 \times L_2,\\
N3_{1200} &= 0.151046 + 1.72268 \times N1_{1200}\\
&\quad - 0.366272 \times N2_{1200} + 0.0388395\\
&\quad \times N1_{1200}^2 - 0.122276 \times N2_{1200}^2\\
&\quad + 0.0151126 \times N1_{1200} \times N2_{1200}\\
&\quad - 0.704662 \times N2_{1200}^3\\
&\quad + 0.259382 \times N2_{1200}^3,\\
TL_{1200} &= 3.65392 + 8.47294 \times N3_{1200}.
\end{aligned}
\tag{9}
$$

In addition, the searching range of $L_1$ and $L_2$ is illustrated in Table 5.

Table 5. Constrained condition in a two-chamber plenum (Case I).

| | Min. [m] | Max. [m] |
|---|---|---|
| $L_1$ | 0.0375 | 0.0625 |
| $L_2$ | 0.085 | 0.115 |

*5.2. CASE II: A three-chamber plenum partitioned with two centre-opening baffles*

As indicated in Fig. 1b, to simplify optimisation, it is assumed that two sets of baffles (with a depth of $LL_1$) located at the horizontal line with a span of $LL_2$ are symmetrical. Two kinds of design parameters – $LL_1$ and $LL_2$ – are chosen as the tuned variables. The *TL*s of the sixteen training data sets shown in Table 2 are calculated by the *BEM*. Using $LL_1$ and $LL_2$ as the input data and the *TL* as the output data in the *NNM*, and inputting a series of training data into the *NNM* system, the fitness functions of the targeted frequencies (400 Hz, 800 Hz, and 1200 Hz) are established and shown below.

**A. Target frequency – 400 Hz**

$$
\begin{aligned}
N1_{400} &= -4.69668 + 46.9668 \times LL_1,\\
N2_{400} &= -5.62917 + 86.6025 \times LL_2,\\
N3_{400} &= 0.35407 - 0.674925 \times N1_{400}\\
&\quad + 0.54201 \times N2_{400} - 0.453741\\
&\quad \times N1_{400}^2 + 0.0760667 \times N2_{400}^2\\
&\quad + 0.0957781 \times N1_{400} \times N2\\
&\quad - 0.206678 \times N1_{400}^3\\
&\quad - 0.290011 \times N2_{400}^3,\\
TL_{400} &= 7.91217 + 3.76395 \times N3_{400}.
\end{aligned}
\tag{10}
$$

**B. Target frequency – 800 Hz**

$$
\begin{aligned}
N1_{800} &= -4.69668 + 46.9668 \times LL_1,\\
N2_{800} &= -5.62917 + 86.6025 \times LL_2,\\
N3_{800} &= 1.08496 - 0.77149 \times N1_{800}\\
&\quad + 0.695113 \times N2_{800} - 1.31996\\
&\quad \times N1_{800}^2 + 0.162666 \times N2_{800}^2\\
&\quad - 0.126623 \times N1_{800} \times N2_{800}\\
&\quad - 0.238903 \times N1_{800}^3\\
&\quad + 0.103649 \times N2_{800}^3,\\
TL_{800} &= 2.35791 + 7.10867 \times N3_{800}.
\end{aligned}
\tag{11}
$$

### C. Target frequency – 1200 Hz

$$
\begin{aligned}
N1_{1200} &= -4.69668 + 46.9668 \times LL_1,\\
N2_{1200} &= -5.62917 + 86.6025 \times LL_2,\\
N3_{1200} &= 0.35895 + 0.74027 \times N1_{1200}\\
&\quad - 0.173428 \times N2_{1200}\\
&\quad + 0.428791 \times N1_{1200}^2\\
&\quad - 0.0459114 \times N2_{1200}^2\\
&\quad + 0.0736646 \times N1_{1200} \times N2_{1200}\\
&\quad + 0134698 \times N1_{1200}^3\\
&\quad - 0.0495031 \times N2_{1200}^3,\\
TL_{1200} &= 0 + 2.63429 + 10.522 \times N3_{1200}.
\end{aligned}
\tag{12}
$$

In addition, the searching range of $LL_1$ and $LL_2$ is illustrated in Table 6.

Table 6. Constrained condition in a three-chamber plenum (Case II).

| | Min. [m] | Max. [m] |
|---|---|---|
| $LL_1$ | 0.0375 | 0.0625 |
| $LL_2$ | 0.05 | 0.08 |

## 6. Results and discussion

### *6.1. Results*

By using the trained *NNM* in conjunction with the *GA* optimiser, a series of optimised results are obtained. The selected *GA* parameters used in Case I and Case II are shown in Table 7. Using a baffle with $\alpha = 0.1$ in Case I, the resulting optimisations with respect to the targeted tones (400, 800, and 1200 Hz) are shown in Table 8. In addition, the resulting optimisations with respect to the targeted tones (400, 800, and 1200 Hz) in Case II using a baffle of $\alpha = 0.1$ are shown in Table 9. Moreover, their *TL* curves, with and without optimisation in Case I, are plotted in Figs. 8–10. Similarly, their *TL* curves, with and without optimisation in Case II, are plotted in Figs. 14–16. As indicated in Table 8, it is obvious that for Case I the acoustical performances (*TL*) at the targeted 400 Hz, 800 Hz, and 800 Hz are improved from 9.3 to 12.6 dB, 21.86 to 27.28, and 10.42 to 16.48 dB. Likewise, as indicated in Table 9, the acoustical performances (*TL*) for Case II at the targeted 400, 800, and 1200 Hz are improved from 7.28 to 12.09 dB, 0.1 to 11.27, and 0.47 to 32.63 dB. To appreciate the influence of the baffle's

Table 7. Selected GA parameters during shape optimisation.

| GA parameters | Value (or condition) |
|---|---|
| design variables | 2 |
| bit | 20 |
| pop | 100 |
| elitism | (tournament) |
| crossover | (uniform crossover) |
| pc | 0.8 |
| pm | 0.05 |
| $\text{iter}_{\max}$ | 1000 |

Table 8. Comparison of acoustical performance with and without shape optimisation at various frequencies (Case I: a two-chamber plenum partitioned with non-sound-absorbing and centre-opening baffles ($\alpha = 0.1$)).

| Targeted frequency | Optimised muffler | | | Original muffler |
|---|---|---|---|---|
| | $L_1$ [m] | $L_2$ [m] | *TL* [dB] | *TL* [dB] |
| 400 Hz | 0.0375 | 0.0853 | 12.6 | 9.3 |
| 800 Hz | 0.061 | 0.1013 | 27.28 | 21.86 |
| 1200 Hz | 0.0598 | 0.1150 | 16.48 | 10.42 |

Note: for original plenum – $L_1 = 0.0375$; $L_2 = 0.0975$

Table 9. Comparison of acoustical performance with and without shape optimisation at various frequencies (Case II: a three-chamber plenum partitioned with non-sound-absorbing and centre-opening baffles ($\alpha = 0.1$)).

| Targeted frequency | Optimised muffler | | | Original muffler |
|---|---|---|---|---|
| | $LL_1$ [m] | $LL_2$ [m] | *TL* [dB] | *TL* [dB] |
| 400 Hz | 0.0375 | 0.0736 | 12.09 | 7.28 |
| 800 Hz | 0.05365 | 0.0501 | 11.27 | 0.1 |
| 1200 Hz | 0.0625 | 0.0815 | 32.63 | 0.47 |

Note: for original plenum – $LL_1 = 0.0375$; $LL_2 = 0.0975$

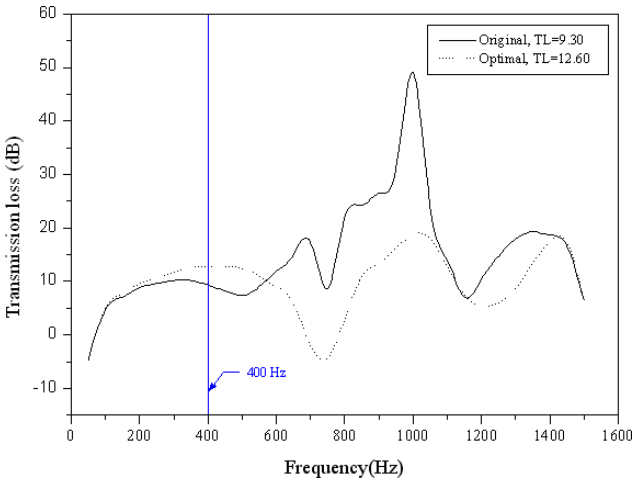


Fig. 8. TL curves with/without optimisation at target 400 Hz [case I: two-chamber plenum partitioned with non-sound-absorbing and centre-opening baffles ($\alpha = 0.1$)].

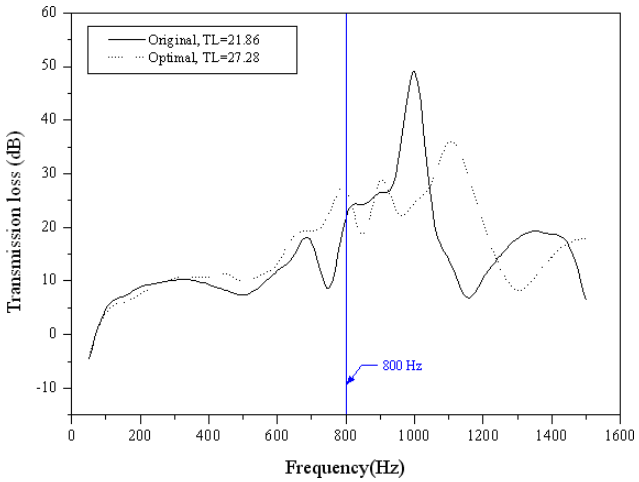


Fig. 9. TL curves with/without optimisation at target 800 Hz [case I: two-chamber plenum partitioned with non-sound-absorbing and centre-opening baffles ($\alpha$=0.1)].

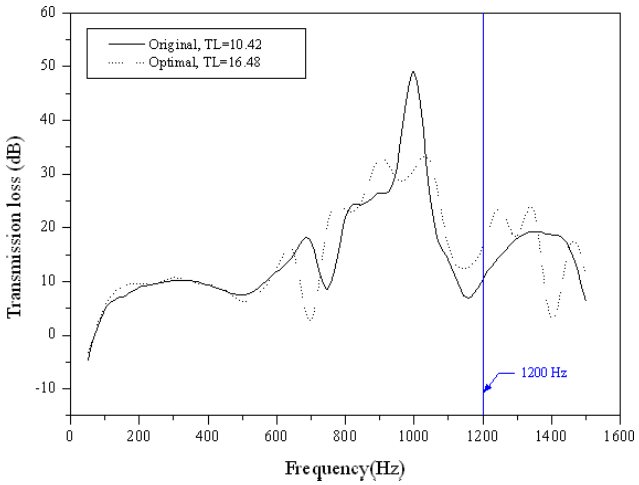


Fig. 10. TL curves with/without optimisation at target 1200 Hz [case I: two-chamber plenum partitioned with non-sound-absorbing and centre-opening baffles ($\alpha$=0.1)].

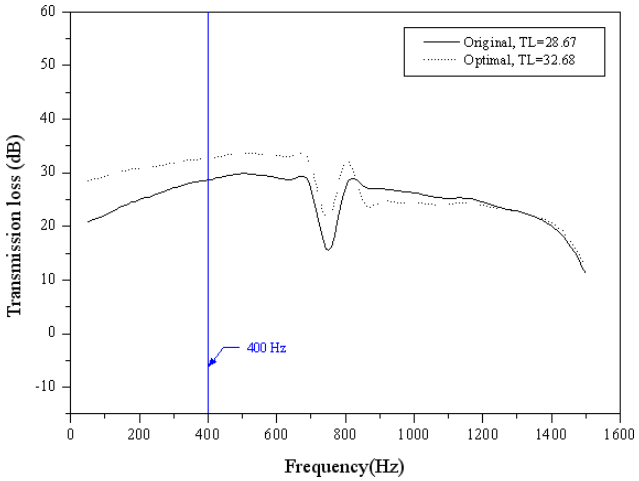


Fig. 11. TL curves with/without optimisation at target 400 Hz [case I: two-chamber plenum partitioned with sound-absorbing and centre-opening baffles ($\alpha = 0.83$)].

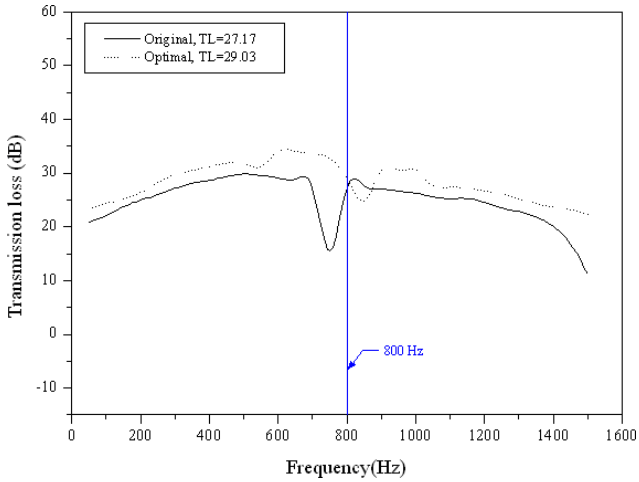


Fig. 12. TL curves with/without optimisation at target 800 Hz [case I: two-chamber plenum partitioned with sound-absorbing and centre-opening baffles ($\alpha = 0.83$)].

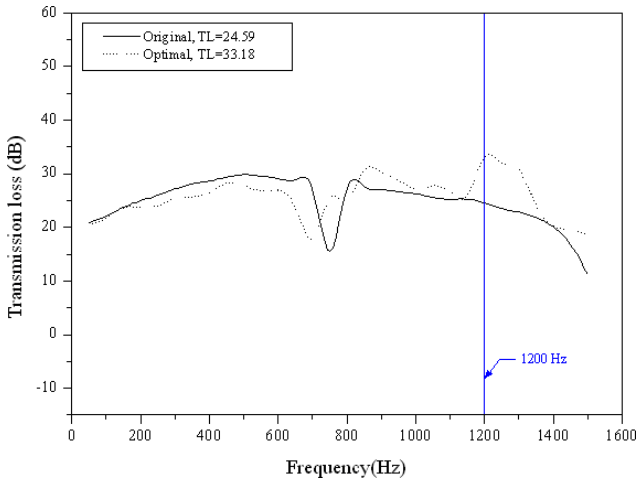


Fig. 13. TL curves with/without optimisation at target 1200 Hz [case I: two-chamber plenum partitioned with sound-absorbing and centre-opening baffles ($\alpha = 0.83$)].

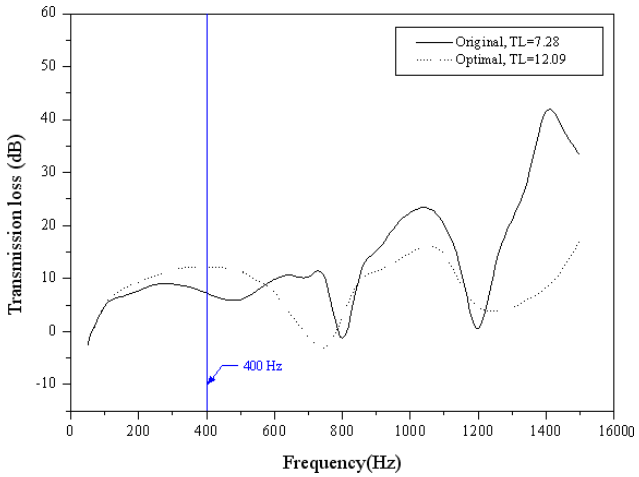


Fig. 14. TL curves with/without optimisation at target 400 Hz [case II: three-chamber plenum partitioned with non-sound-absorbing and centre-opening baffles ($\alpha = 0.1$)].

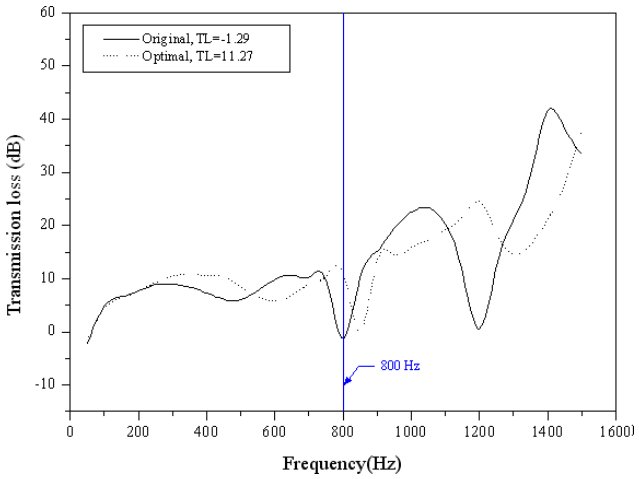


Fig. 15. TL curves with/without optimisation at target 800 Hz [case II: three-chamber plenum partitioned with non-sound-absorbing and centre-opening baffles ($\alpha = 0.1$)].

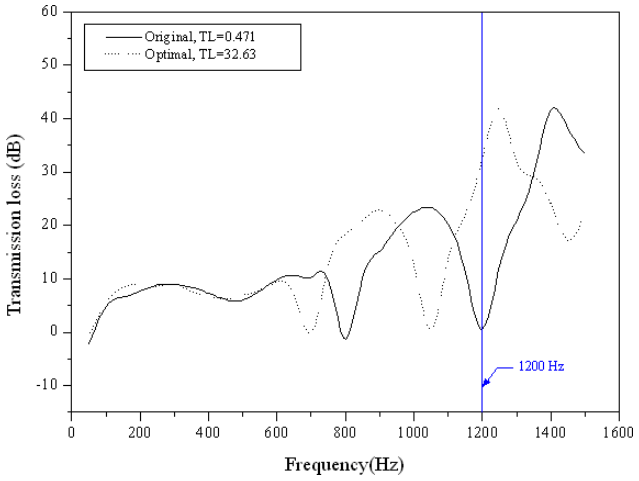


Fig. 16. TL curves with/without optimisation at target 1200 Hz [case II: three-chamber plenum partitioned with non-sound-absorbing and centre-opening baffles ($\alpha = 0.1$)].

sound absorption coefficient on the plenum's $TL$, using a baffle with $\alpha = 0.83$ in Case I and Case II, the resulting $TL$ in the two-chamber and three-chamber plenums are shown in Table 10 and Table 11. As indicated in Table 10, the acoustical performances ($TL$) for Case I at the targeted 400, 800, and 1200 Hz are

Table 10. Comparison of optimal acoustical performance of various sound absorption coefficients at various frequencies (Case I: a two-chamber plenum partitioned with non-sound-absorbing ($\alpha = 0.1$) and sound-absorbing ($\alpha = 0.83$) centre-opening baffles).

| Targeted frequency | $TL$ of optimised muffler [dB] | |
|---|---|---|
| | $\alpha = 0.1$ | $\alpha = 0.83$ |
| 400 Hz | 12.6 | 32.68 |
| 800 Hz | 27.28 | 29.03 |
| 1200 Hz | 16.48 | 33.18 |

Table 11. Comparison of optimal acoustical performance of various sound absorption coefficients at various frequencies (Case II: a three-chamber plenum partitioned with non-sound-absorbing ($\alpha = 0.1$) and sound-absorbing ($\alpha = 0.83$) centre-opening baffles).

| Targeted frequency | $TL$ of optimised muffler [dB] | |
|---|---|---|
| | $\alpha = 0.1$ | $\alpha = 0.83$ |
| 400 Hz | 12.09 | 34.31 |
| 800 Hz | 11.27 | 33.54 |
| 1200 Hz | 32.63 | 33.24 |

32.68 dB, 29.03 dB, and 33.18 dB. Similarly, as indicated in Table 11, the acoustical performances ($TL$) for Case II at the targeted 400, 800, and 1200 Hz are 34.31 dB, 33.54 dB, and 33.24 dB.

### *6.2. Discussion*

For the two-chamber plenum, as indicated in Table 8, the best acoustical performances of the targeted tones (400 Hz, 800 Hz, and 1200 Hz) are 12.6–27.28 dB. Based on the selected targeted frequency, the design parameters, $L_1$ and $L_2$, will be adjusted during the $GA$ optimisation. Figures 8–10 indicate that the $TL$s are roughly maximized around the desired frequency. In addition, the acoustical performance within a range of 800–1100 Hz will be remarkable.

Similarly, for the three-chamber plenum, as indicated in Table 9, the best acoustical performance of the targeted tones (400 Hz, 800 Hz, and 1200 Hz) is 11.27–32.63 dB. Depending on the selected targeted frequency, the design parameters, $LL_1$ and $LL_2$, will be adjusted during the $GA$ optimisation. Figures 14–16 indicate that the $TL$s are roughly maximised around the desired frequency. In addition, the profile of the $TL$s within a range of 700–1000 Hz and 1000–1500 Hz will be remarkable.

As can be noted, the acoustical performances of a two-chamber plenum lined with sound absorbing material ($\alpha = 0.83$) at various targeted tones (400, 800, and 1200 Hz) are assessed and plotted in Figs. 11–13. As indicated in Figs. 11–13, the profile of the $TL$s within a range of 100 Hz to 1500 Hz are promoted and broadened. The comparison of the acoustical performance of a two-chamber plenum before and after using sound absorbing material is shown in Table 10. Table 10 reveals that the $TL$s at the targeted tones (400 Hz, 800 Hz, and 1200 Hz) will be improved from 12.6 to 32.68 dB, 27.28 to 29.03 dB, and 16.48 to 33.18 dB when using the sound absorbing material ($\alpha = 0.83$).

Likewise, the acoustical performance of a three-chamber plenum at various targeted tones (400, 800, and 1200 Hz) is assessed and plotted in Figs. 17–19 when using sound absorbing material ($\alpha = 0.83$) on

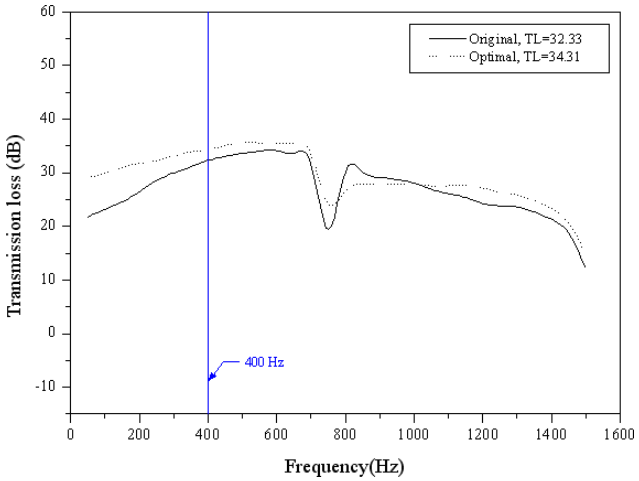


Fig. 17. TL curves with/without optimisation at target 400 Hz [case II: three-chamber plenum partitioned with sound-absorbing and centre-opening baffles ($\alpha = 0.83$)].

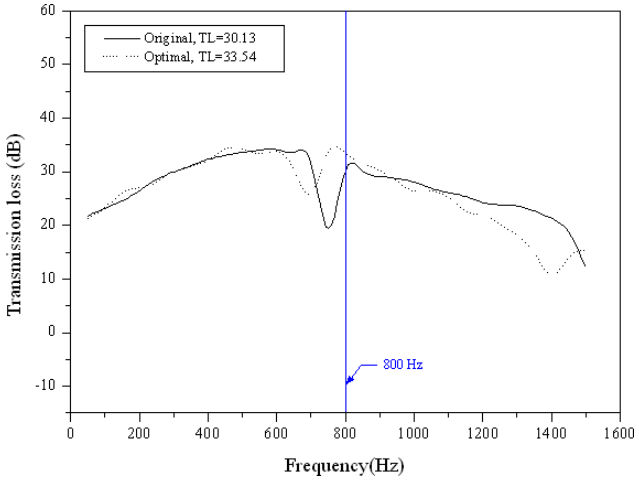


Fig. 18. TL curves with/without optimisation at target 800 Hz [case II: three-chamber plenum partitioned with sound-absorbing and centre-opening baffles ($\alpha = 0.83$)].

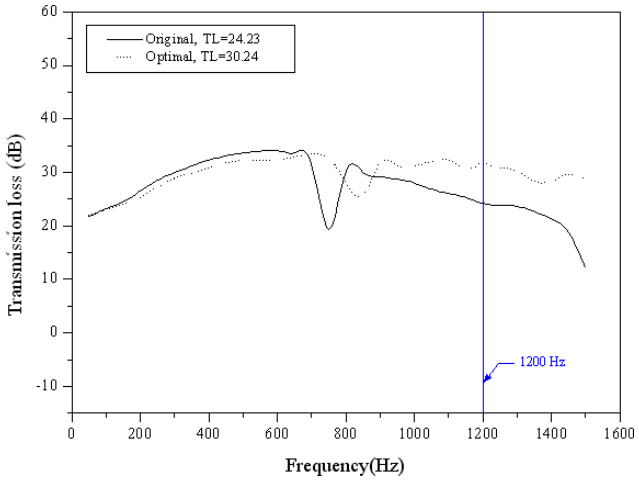


Fig. 19. TL curves with/without optimisation at target 1200 Hz [case II: three-chamber plenum partitioned with sound-absorbing and centre-opening baffles ($\alpha = 0.83$)].

the baffles. As indicated in Figs. 17–19, the profile of the *TL*s within a range of 100 Hz to 1500 Hz is also promoted and broadened. The comparison of the acoustical performance of a three-chamber plenum before and after using sound absorbing material is shown in Table 11. Table 11 reveals that the *TL*s at the targeted tones (400 Hz, 800 Hz, and 1200 Hz) will be improved from 12.09 to 34.31 dB, 11.27 to 33.54 dB, and 32.63 to 33.24 dB when using sound absorbing material ($\alpha = 0.83$).

Subsequently, as indicated in Table 10 and Table 11, the acoustical performance of a three-chamber plenum is a little bit higher than that of the two-chamber plenum when the sound absorbing material ($\alpha = 0.83$) is applied. The results reveal that the acoustical performances for Case I and Case II are almost identical. This is because the centre-opening baffles for Case I and Case II are on the same centre line. Therefore the sound wave emitted from the first layer of the baffle will transmit directly into the next opening of the second layer of the baffle. Moreover, the back pressure of the three-chamber plenum will be higher than that of the two-chamber plenum. Consequently, considering the back pressure effect, the design of the two-chamber plenum will be better than that of the three-chamber plenum.

## 7. Conclusion

The present paper indicates that a multi-chamber plenum can be roughly optimised at a targeted frequency with the *NNM* and the *GA* method by adjusting the plenum baffle's shape within the space constraints. When using the polynomial neural network instead of the complicated mathematical model (*BEM*), the design parameters can be easily changed without a total overhaul of the plenum design; therefore, the surrogate model – a trained neural network model (*NNM*) fitted with a series of real data – can be established and used as a new *OBJ* function. Before optimisation is performed, the accuracy of the boundary element method (*BEM*) for a three-chamber plenum is checked by experimental data and found to be accurate. Because the real data are very close to the *BEM* data and to facilitate the assessment of real data fit to a *NNM*, the *BEM* data are used as the real data. Moreover, for two kinds of plenums (two-chamber and three-chamber), the similarity of the *TL* related to the *BEM* and *NNM* at various targeted tones is sufficient. Furthermore, the optimal values of the *TL* achieved at the target frequencies reveal that the *NNM* along with the *GA* optimiser for two kinds of plenums (two-chamber and three-chamber ones) are applicable. The results reveal that for the two-chamber and three-chamber plenums, the profile of the *TL*s within a range of 100 Hz to 1500 Hz is promoted and broadened when using baffles lined with sound absorbing material

($\alpha = 0.83$) at various targeted tones (400, 800, and 1200 Hz).

As indicated in Figs. 8–10 and Figs. 14–16, the profiles reveal that for the two-chamber and three-chamber plenums, the acoustical performance within a range of 800–1100 Hz and 700–1500 Hz will be remarkable. Beyond those frequencies, the acoustical performance will become lower. The results reveal that the acoustical performances for Case I and Case II are almost the same when the baffles are lined with sound-absorbing material ($\alpha = 0.83$). Moreover, the back pressure of the three-chamber plenum will be higher than that of the two-chamber plenum.

As it can be observed in Fig. 1, an optimal multi-chamber plenum is efficient when used to deal with a steady industrial piping noise at various targeted tones. It can also be seen that the construction fee for a simple geometric multi-chamber plenum is much lower than that of a traditional reactive muffler. Therefore, the use of an optimised multi-chamber plenum in industry is seen to be much more advantageous.

Consequently, the use of the *GA* optimisation in conjunction with *NNM* and *BEM* in the multi-chamber plenum's baffle shape design is more efficient than the complicated models (transfer matrix and analytical methods) or redundant tests conducted in the laboratory.

## References

1. Alley B.C., Dufresne R.M., Kanji N., Reesal M.R. (1989), *Costs of workers' compensation claims for hearing loss*, Journal of Occupational Medicine, **31**, 134–138.
2. Bie D.A., Hansen C.H. (1988), *Engineering noise control: theory and practice*, Unwin Hyman, London.
3. Blair G.P., Coates S.W. (1973), *Noise produced by unsteady exhaust efflux from an internal combustion engine*, *SAE*, 73160.
4. Chang Y.C., Yeh L.J., Chiu M.C. (2004), *Numerical studies on constrained venting system with side inlet/outlet mufflers by GA optimisation*, Acta Acustica united with Acustica, **1**, 1–11.
5. Chang Y.C., Yeh L.J., Chiu M.C. (2005a), *Shape optimisation on double-chamber mufflers using Genetic Algorithm*, Proc. ImechE Part C: Journal of Mechanical Engineering Science, **10**, 31–42.
6. Chang Y.C., Yeh L.J., Chiu M.C., Lai G.J. (2005b), *Shape optimisation on constrained single-layer sound absorber by using GA method and mathematical gradient methods*, Journal of Sound and Vibration, **286**, 4–5, 941–961.
7. Cheremisinoff P.N., Cheremisinoff P.P. (1977), *Industrial noise control handbook*, Ann Arbor Science, Michigan.
8. Chiu M.C. (2010), *Shape optimisation of one-chamber Mufflers with reverse-flow ducts using a genetic algorithm*, Journal of Marine Science and Technology, **18**, 1, 12–23.
9. Chiu M.C., Chang Y.C. (2008), *Numerical studies on venting system with multi-chamber perforated mufflers by GA optimisation*, Applied Acoustics, **69**, 11, 1017–1037.
10. Chiu M.C., Chang Y.C. (2010), *Numerical assessment of a space-constrained venting system with multi-chamber plug mufflers by GA method*, Journal of Marine Science and Technology, **18**, 3, 317–332.
11. Ffowcs J.E., Howe M.S. (1975), *The generation of sound by density inhomogenities in low mach number nozzle flows*, J. of Fluid Mechanics, **70**, 3, 605–622.
12. Holland J. (1975), *Adaptation in natural and artificial system*, Ann Arbor, University of Michigan Press.
13. Ivakhnenko A.G. (1971), *Polynomial theory of complex system*, IEEE Trans. Syst. Man. Cyber, **1**, 4, 364–368.
14. Jong D. (1975), *An analysis of the behavior of a class of genetic adaptive systems*, Doctoral Dissertation, Department of Computer and Communication Sciences, Ann Arbor, University of Michigan, USA.
15. Ko S.H. (1971), *Sound attenuation in lined rectangular ducts with flow and its application to the reduction of aircraft engine noise*, J. Acoust. Soc. Am., **50**, 6, 1418–1432.
16. Laurence W. (1998), *Integer programming*, John Wiley & Sons, New York.
17. Li X., Hansen C.H. (2005), *Comparison of models for predicting the transmission loss of plenum chambers*, Applied Acoustics, **66**, 7, 810–828.
18. Liu J., Herrin D.W. (2010), *Enhancing micro-perforated panel attenuation by partitioning the adjoining cavity*, Applied Acoustics, **71**, 120–127.
19. Mccormick A.M. (1975), *The attenuation of sound in lined rectangular ducts containing uniform Flow*, Journal of Sound and Vibration, **39**, 1, 35–41.
20. Munjal M.L. (1997), *Plane wave analysis of side inlet/outlet chamber mufflers with mean flow*, Applied Acoustics, **52**, 165–175.
21. Patrikar A., Provence J. (1996), *Nonlinear system identification and adaptive control using polynomial networks*, Mathl. Comput. Modeling, **23**, 1/2, 159–173.
22. Rardin R.L. (1998), *Optimisation in operations research*, Prentice Hall, New Jersey.
23. Yeh L.J., Chang Y.C., Chiu M.C. (2006), *Numerical studies on constrained venting system with reactive mufflers by GA optimisation*, International Journal for Numerical Methods in Engineering, **65**, 1165–1185.
24. Yeh L.J., Chang Y.C., Chiu M.C., Lai G.J. (2004), *GA optimisation on multi-segments muffler under space constraints*, Applied Acoustics, **65**, 5, 521–543.